

Effect of Nb on Microstructural Characteristics of Ti–Nb–Ta–Zr Alloy for Biomedical Applications

Shujun Li¹, Yulin Hao¹, Rui Yang¹, Yuyou Cui¹ and Mitsuo Niinomi²

¹Institute of Metal Research, Chinese Academy of Sciences, 72 Wenhua Road, Shenyang 110016, P.R. China

²Department of Production Systems Engineering, Toyohashi University of Technology, Toyohashi 441-8580, Japan

The effects of several commonly used heat treatment schemes on the microstructures of two Ti–Nb–Ta–Zr alloys aimed at biomedical applications were studied in this work using scanning electron microscopy (SEM) and transmission electron microscopy (TEM). The specimens were water quenched from 790°C and then aged at temperatures between 300°C and 600°C. The experimental results showed that α and ω phase precipitated from the metastable β matrix in Ti–29Nb–13Ta–4.6Zr alloy during isothermal ageing. But for Ti–39Nb–13Ta–4.6Zr, the precipitation reaction was more sluggish than that in Ti–29Nb–13Ta–4.6Zr because of high amount of β stabilizing elements in the former alloy. As a result the α phase was unable to precipitate during short time ageing treatment. After longer time (12 days) ageing treatment at 500°C or 400°C, recognizable α precipitates were observed in the aged samples. It is concluded that Ti–29Nb–13Ta–4.6Zr can be heat treated to obtain different microstructures and is better than Ti–39Nb–13Ta–4.6Zr in terms of age hardenability.

(Received April 16 2002; Accepted July 19, 2002)

Keywords: titanium–niobium–tantalum–zirconium alloy, biomaterial, microstructure, phase transformation

1. Introduction

Titanium alloys are a favorable choice for orthopedic implant applications, as they possess good mechanical properties and biochemical compatibility. For example, Ti–6Al–4V ELI, Ti–5Al–2.5Fe, and Ti–6Al–7Nb developed for such purposes have found wide applications.^{1–3} However, toxicity of the elements Al and V in these alloys has been noted.^{4,5} In addition, these alloys are still too stiff compared to human bone, which may lead to premature failure of the implant.

Biomechanical compatibility requires high permissible elastic strain, *i.e.*, the strength to modulus ratio, so an ideal material should have high strength but low modulus. As far as low modulus is concerned, β titanium alloy is advantageous. The theoretical studies of Song *et al.* suggest that Zr, Nb, Mo, Hf, and Ta are suitable to increase the strength and decrease the modulus of bcc Ti.^{6,7} As to the toxicity of elements, Nb, Mo, Hf and Ta are the least toxic and are therefore the most suitable alloying elements for β -type titanium alloys. So the biomedical titanium alloys developed recently mainly contain Ti, Nb, Ta, Zr.^{8–11}

In Japan, a new alloy, Ti–29Nb–13Ta–4.6Zr, has recently been developed that possesses low modulus and low strength under the condition of solution treatment followed by quenching (STQ).⁹ Biomedical application of the alloy requires further optimization of the strength to modulus ratio. For similar alloy families, it has been reported that the strength and Young's modulus are dependent on the microstructure and Nb content.^{12–16} It is therefore of interest to examine how the microstructure of Ti–Nb–Ta–Zr alloy is affected by variation in the Nb content, and how the change in composition affects the kinetics of phase transformation during heat treatment. The purpose of the present study was to compare the phase transformation during solution treatment and precipitation phenomena during subsequent ageing between Ti–29Nb–13Ta–4.6Zr and an alloy with much higher Nb content, Ti–39Nb–13Ta–4.6Zr.

2. Experimental

The Ti–29Nb–13Ta–4.6Zr ingot with a diameter of 60 mm was fabricated by induction skull melting using pure Ti, Nb, Ta and Zr as raw materials and then hot forged to rods with a diameter of 20 mm. The ingot of Ti–39Nb–13Ta–4.6Zr was prepared by first melting in an electron beam melter using raw materials of pure Ti, Nb, Ta and Zr, and then by remelting in a vacuum arc remelting furnace. The ingot was then forged at 850°C to a rod 24 mm in diameter. The actual compositions of all the alloys obtained by wet chemical analysis are shown in Table 1.

Cylindrical sections 25 mm in length were taken from the two alloy rods (with diameters of 20 and 24 mm) for the investigations. Specimens were first solution treated at 790°C for 1 h followed by water quenching. Then, these solution treated specimens were aged at 300, 350, 400, 450, 500 or 600°C for 48 h, and then quenched into water. Some of the Ti–39Nb–13Ta–4.6Zr specimens were aged at 400 or 500°C for 12 days to facilitate the precipitation reaction.

The microstructures were observed with a JSM-6301F scanning electron microscope (SEM) and a Philips EM420 transmission electron microscope (TEM) operating at 100 kV. The specimens for the SEM analysis were mechanically polished and then etched in a solution consisting of 8 vol% HF, 15 vol% HNO₃ and 77 vol% H₂O. Samples for TEM analysis were prepared from mechanically thinned plates by ion

Table 1 Chemical compositions of the forged Ti–29Nb–13Ta–4.6Zr and Ti–39Nb–13Ta–4.6Zr (mass%).

Alloy	Compositions					
	Nb	Ta	Zr	O	N	Ti
Ti–29Nb–13Ta–4.6Zr	30.2	12.4	4.8	0.16	0.01	bal.
Ti–39Nb–13Ta–4.6Zr	39.8	13.5	5.0	0.088	0.015	bal.

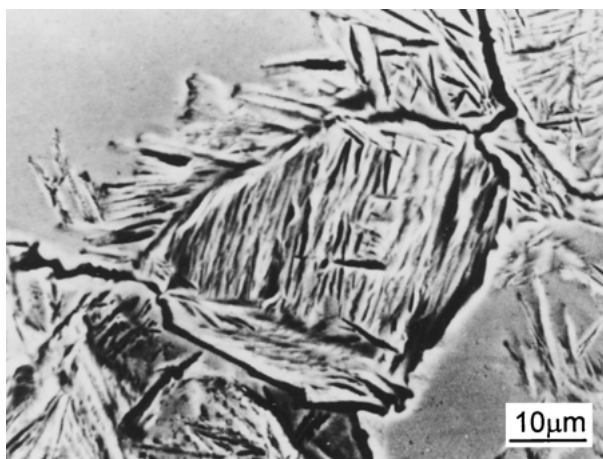


Fig. 1 SEM micrograph of as-quenched Ti–29Nb–13Ta–4.6Zr, showing the morphology of α'' martensite in a β matrix.

milling with 5 keV argon ions at an angle of incidence of 15 degrees.

3. Results

3.1 Microstructures of as quenched alloys

Figure 1 shows an SEM micrograph of ($\beta + \alpha''$) microstructure of Ti–29Nb–13Ta–4.6Zr alloy solution treated at 790°C for 1 h followed by water quenching. X-ray diffraction analysis showed the presence of (020), (111) and (113) peaks of orthorhombic α'' martensite formed during fast cooling in the water quenched specimens. For Ti–39Nb–13Ta–4.6Zr, no evidence of orthorhombic α'' martensite was observed in the as-quenched condition. For both alloys, diffuse scattering was observed on the selected area electron diffraction (SAD) patterns of the β phase in the as quenched state, although it is stronger in the high Nb alloy than in the low Nb alloy. Diffuse scattering by electrons is a common phenomenon for many derivatives of the body-centred cubic structure, and may be due to a variety of static or dynamic causes. In the present alloy system, the most likely explanation of the abnormal scattering is precursor of the athermal transformation to the ω structure. The formation of ω_{ath} (the subscription denotes athermal) is a displacement-controlled reaction, and short-range-correlated displacements resulting from the collapse of the (111) $_{\beta}$ planes give rise to the diffuse streaks and displacement of the reflections from their ideal positions.^{17,18)} For the high Nb alloy in the as quenched state, the diffuse maxima are shifted away from the ideal positions of the ω phase (see Fig. 2), indicating that the athermal transformation was still in an early stage. Attempts at direct observation of the ω phase particles in this condition were not successful, either from dark field (DF) images using the diffuse streaks nor from bright field (BF) images. For as quenched Ti–29Nb–13Ta–4.6Zr alloy, the diffuse streaks are weaker and more uniform, and diffuse maxima have not formed yet. Previous studies^{19,20)} showed that the formation of ω_{ath} phase is sensitive to alloy composition and cooling rate, so a low Nb concentration and fast cooling rate (WQ), together with the formation of the α'' martensite, may have helped in preventing the precipitation of ω_{ath} from Ti–29Nb–13Ta–4.6Zr alloy.

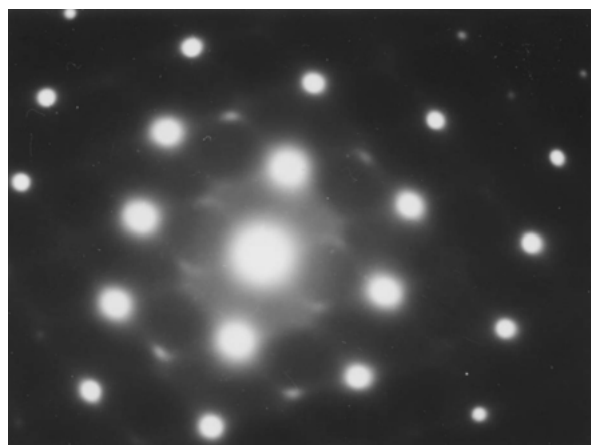


Fig. 2 $\langle 110 \rangle_{\beta}$ SAD pattern of as-quenched Ti–39Nb–13Ta–4.6Zr.

3.2 Microstructures of aged alloys

Results show that the ageing treatments exert great effects on the microstructures of Ti–29Nb–13Ta–4.6Zr alloy. The isothermal precipitation of the ω phase was observed in the specimens aged at 400, 350 or 300°C for 2 days. The dark-field transmission electron micrograph shows that the ω phase particles formed during isothermal reaction have ellipsoidal shape and distribute uniformly in the β grains (see Fig. 3(a)). The SAD pattern obtained from $\langle 110 \rangle_{\beta}$ zone axis is shown in Fig. 3(b) and indexed in Fig. 3(c). The discrete reflections at positions such as $2/3\langle 211 \rangle$ and $1/3\langle 111 \rangle$ in the diffraction pattern are due to the formation of isothermal ω -type phase in the aged alloy. de Fontaine *et al.*¹⁷⁾ concluded that, in contrast to short-range correlated displacements, the displacement mode for isothermal ω -type phase is long range, giving rise to sharp ω reflections. The positions of these reflections in the current study are consistent with the disordered, hexagonal ω -type transformation; the orientation relationship between the bcc matrix and the ω -type phase can be determined as $(0001)_{\omega} // (111)_{\beta}$ and $[11\bar{2}0]_{\omega} // [011]_{\beta}$, which is in agreement with the results published by Silcock *et al.* (cited in Ref. 21)). Precipitation of the α phase was observed in the Ti–29Nb–13Ta–4.6Zr samples aged at 600, 500, 450, 400, or 350°C for two days. The morphology of the α particles is needle-like (see Fig. 4(a)). An SAD pattern from $\langle 111 \rangle_{\beta}$ taken from regions containing precipitates (Fig. 4(a)) is shown in Fig. 4(b). The orientation relationship between the α phase and the β phase can be determined as $\langle 111 \rangle_{\beta} // \langle 11\bar{2}0 \rangle_{\alpha}$, which obeys the Burgers orientation relationship.²²⁾ Increasing the ageing temperature caused coarsening of the precipitates and decrease in their number. The precipitation of the α phase initiates simultaneously at the grain boundaries and within the grains, although grain boundaries appear to be preferred nucleation sites, see Fig. 5.

For Ti–39Nb–13Ta–4.6Zr alloy, by contrast, after ageing at 300, 350, 400, 450, 500, or 600°C for two days, no definite α reflections were observed in the SAD patterns. Only very faint and streaked ω reflections were observed in the samples aged at 300, 350, or 400°C. Some precipitates were found in the bright field image of the samples aged at 300, 350, 400, 450, or 500°C (see Fig. 6(a)). SAD patterns taken from regions containing appreciable amounts of the precipitate show only β -phase reflections and no additional spots due to a sec-

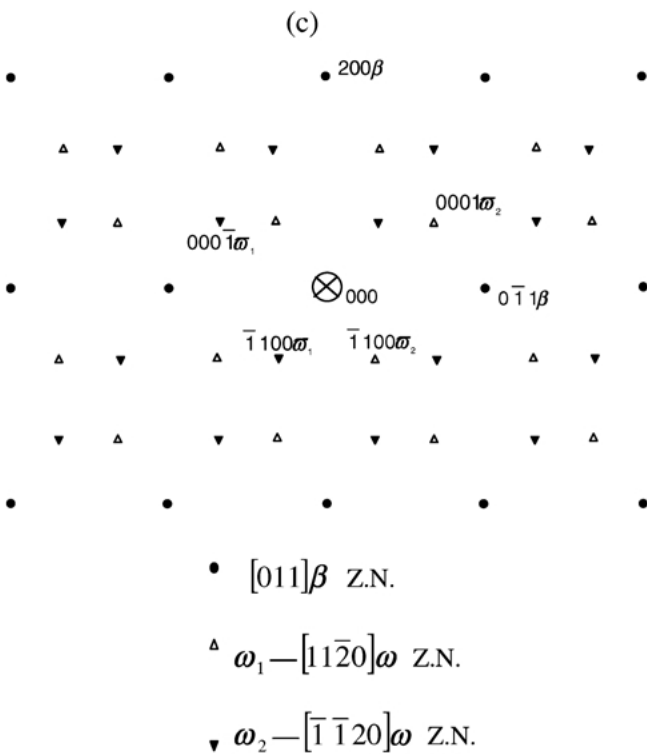
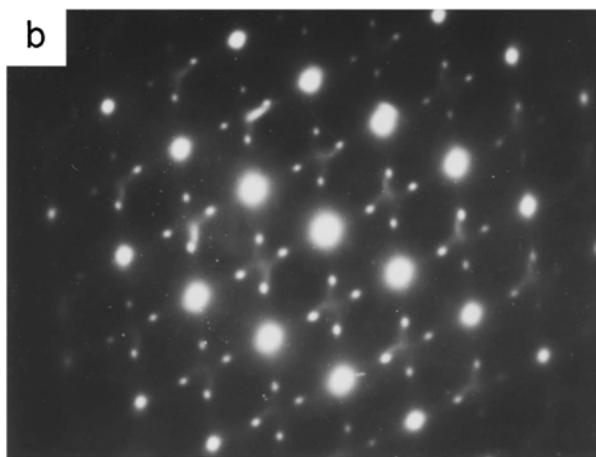
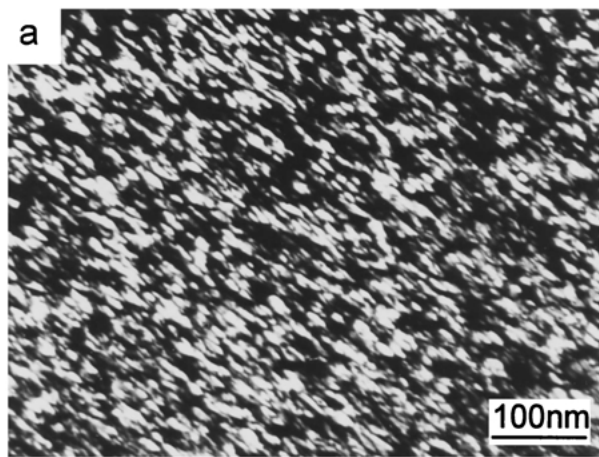


Fig. 3 Dark field TEM micrograph (a), $(110)_\beta$ SAD pattern (b) and an indexed diffraction pattern (c) of Ti-29Nb-13Ta-4.6Zr quenched and then aged at 300°C for two days.

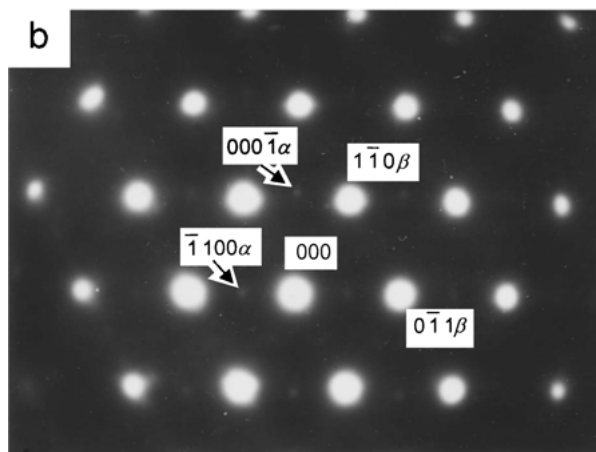
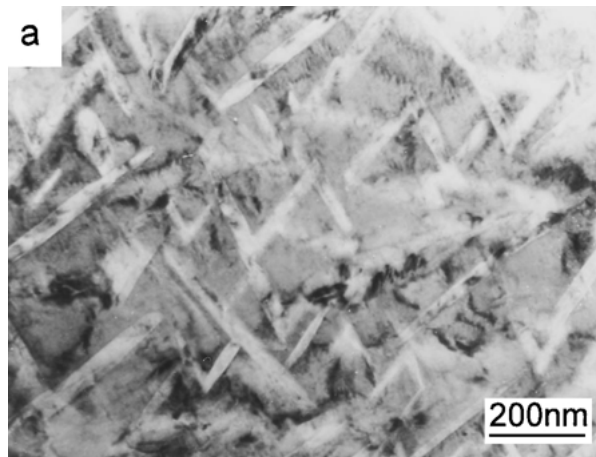


Fig. 4 (a) Bright field TEM micrograph of Ti-29Nb-13Ta-4.6Zr quenched and then aged at 500°C for two days; (b) $(111)_\beta$ SAD pattern showing the superimposed patterns from β and α phases.

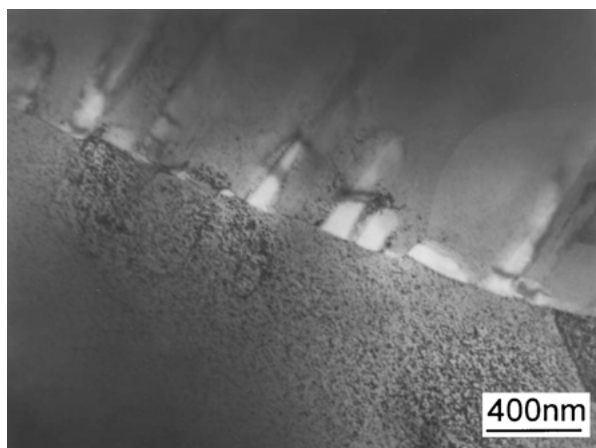


Fig. 5 Bright field TEM micrograph showing the nucleation of the α phase from a grain boundary in Ti-29Nb-13Ta-4.6Zr quenched and then aged at 600°C for two days.

ond phase in the sample (see Fig. 6(b)). After ageing at 500 or 400°C for 12 days, some coarse plate-like precipitates were observed in Ti-39Nb-13Ta-4.6Zr alloy (see Fig. 7(a)). The corresponding SAD pattern shows that these precipitates belong to the α phase (see Fig. 7(b)).

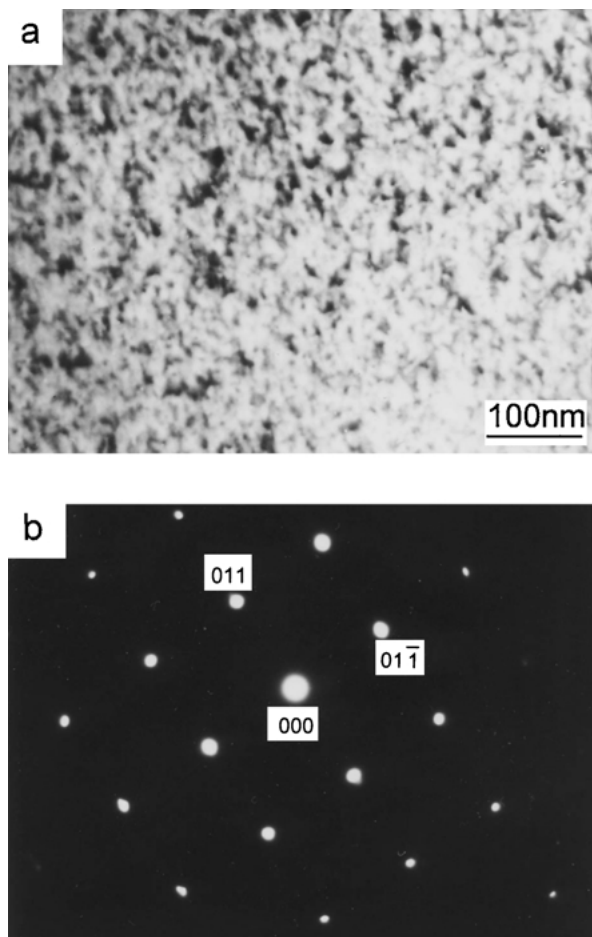


Fig. 6 Bright field TEM micrograph (a) and $\langle 100 \rangle_{\beta}$ SAD pattern (b) of Ti–39Nb–13Ta–4.6Zr quenched and then aged at 500°C for two days.

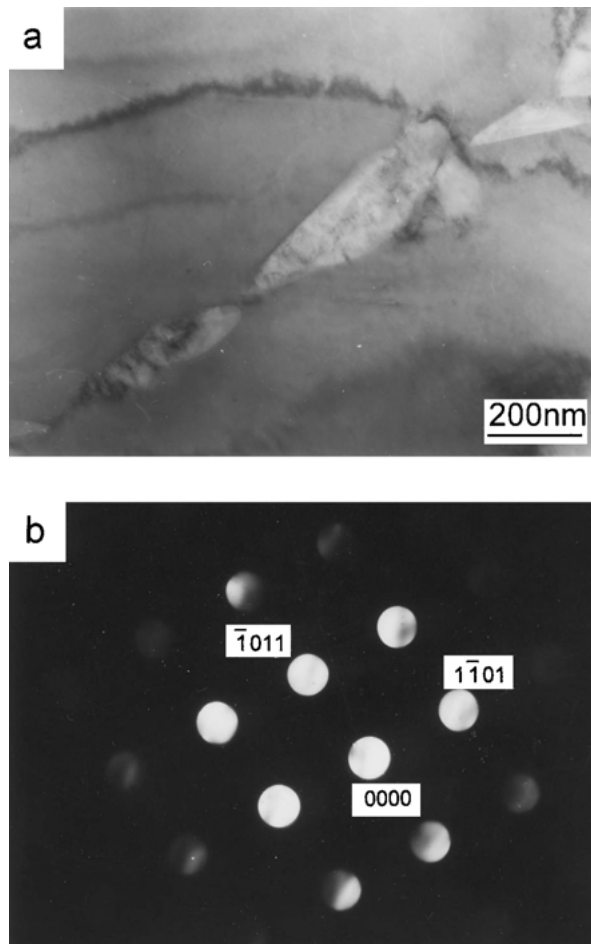


Fig. 7 Bright field TEM micrograph (a) and $\langle 12\bar{3}1 \rangle_{\alpha}$ SAD pattern (b) of Ti–39Nb–13Ta–4.6Zr quenched and then aged at 500°C for twelve days.

4. Discussion

This investigation has shown that the phase transformations observed in Ti–Nb–Ta–Zr alloys are strongly related to the Nb content. According to Kaufman's results on the martensitic starting temperature (M_s) of Ti–Nb alloys,²³ M_s is a function of Nb content, and it decreases with increase in Nb. The M_s for 29 mass% and 39 mass% Nb is about 300 and 100°C, respectively. In the study of Moffat and Larbalestier,²⁴ α'' was observed in alloys with the two compositions. In this study, α'' still appeared in Ti–29Nb–13Ta–4.6Zr (despite extra alloying with Ta and Zr) but not in Ti–39Nb–13Ta–4.6Zr. It is known that the addition of β stabilizing elements decreases the M_s and hence decreases the α'' volume fraction.^{11,24} Therefore, high content of Nb in combination with a significant amount of another β stabilizing element (Ta) has contributed to the stability of the β phase and prohibited the formation of the α'' in quenched Ti–39Nb–13Ta–4.6Zr.

The stabilizing effect on the β phase of the high Nb content appears to promote the formation of athermal ω phase, in contrast to its influence on the formation of α'' and α . This is supported by the stronger evidence of ω_{ath} phase for the high Nb alloy presented in Section 3.1. Athermal formation involves a displacive mechanism, that is, it occurs by collapse of atomic planes within the parent phase. Since no solute diffusion is necessary for the formation of ω_{ath} , it occurs as soon

as the thermodynamic driving force is sufficient to initiate the collapse of the crystallographic planes.^{17,18} This is the reason why diffuse maxima close to the position of the ω phase was present on the SAD patterns of the high Nb alloy, although solute diffusion is very difficult in this alloy, as evidenced by the very slow kinetics of α precipitation.

The experimental results show that the microstructure of Ti–29Nb–13Ta–4.6Zr is sensitive to ageing treatment, with the precipitation of both the α phase and the ω phase during ageing between 600 and 300°C. The high Nb alloy, Ti–39Nb–13Ta–4.6Zr, is more stable than Ti–29Nb–13Ta–4.6Zr. After ageing treatment for relatively short time (two days), definite evidence of α phase and isothermal ω phase was not observed from bright field TEM image of the high Nb alloy. Instead, precipitation similar to the formation of a $\beta + \beta'$ structure^{25,26} was found in these aged specimens (see Fig. 6(a)). In the study of another β titanium alloy, Narayanan and Archbold²⁶ argued that when sufficient β stabilizing additions are present to retain β to room temperature, solute segregation or β -phase separation would occur during ageing. This decomposition mechanism can result in the formation of a β phase that is rich in β stabilising element, *i.e.*, β' . Moffat and Larbalestier,²⁴ on the other hand, believed that these unidentifiable precipitates are α nuclei. Our experimental results seem to support the argument of Moffat and Larbalestier, because long time ageing of the Ti–39Nb–13Ta–4.6Zr specimens at 500 or

400°C produced recognizable α phase (see Fig. 7).

It is notable that the oxygen content of Ti–29Nb–13Ta–4.6Zr is about two times that of Ti–39Nb–13Ta–4.6Zr alloy. Because oxygen stabilizes the α phase, the higher content of oxygen may cause faster kinetics of α precipitation in Ti–29Nb–13Ta–4.6Zr alloy. Increasing oxygen content has similar effect to decreasing Nb content on the β transus temperature because Nb is a β stabilizer. The influence of Nb, Ta, Zr and O on the β transus temperature can be evaluated using the following equation:²⁷⁾

$$T(^{\circ}\text{C}) = 885 - 8.5[\text{Nb}] - 1[\text{Ta}] - 2[\text{Zr}] + 200[\text{O}]$$

where the element in square brackets denotes its concentration by mass percentage in the alloy. Using this equation, the β transus temperature of the low Nb alloy is estimated to be higher by about 96°C than that of the high Nb alloy, whereas the contribution due to the difference in oxygen content between the two alloys is 14.4°C, about 15% of the total effect due to both Nb and oxygen. The foregoing discussion suggests that the influence due to different oxygen levels on the precipitation of the α phase is small compared to that due to the difference in Nb content.

The above argument is based on the assumption that the formation of the α phase is thermodynamically possible in both alloys. Because the oxygen content of the high Nb alloy is only about half that of the low Nb alloy, it is possible that the formation of the α phase is almost completely suppressed in the low Nb alloy which then falls out of the age-hardening category. The relative contributions of the kinetic and thermodynamic factors in delaying and suppressing the precipitation of the α phase in this class of alloys await further clarification.

As mentioned in the introduction section, the strength and Young's modulus of an alloy are related to the relative amount of its constituent phases. After ageing treatment, three phases (α , β and ω) are present in the two Ti–Nb–Ta–Zr alloys. Of these phases the ω has high Young's modulus and low ductility, so attention should be paid to the $\alpha + \beta$ microstructure. Compared to the β phase, the α phase is harder²⁸⁾ and possesses higher Young's modulus.^{29,30)} The Young's modulus of the low Nb alloy was found to be sensitive to the volume fraction of the α phase,²⁸⁾ and the strength of the alloy could be modified by changing the volume fraction of the hard phase,³¹⁾ so adjusting the volume fraction of the α phase by ageing treatment is a possible way to balance the Young's modulus with tensile properties for optimal mechanical compatibility with human bone. Further research regarding the effect of the volume fraction of the α phase on the Young's modulus and strength of the two Ti–Nb–Ta–Zr alloys are in progress in the authors' laboratories.

The present experimental work shows that short time (up to 2 days) ageing treatment exerts little influence on the microstructure of Ti–39Nb–13Ta–4.6Zr. The precipitation of the α phase that is needed to improve the strength of the alloy is largely suppressed and does not occur at a practical rate, owing to the high concentration of β stabilizing elements and the relatively low oxygen content (which promotes the α phase). Therefore, as far as microstructural response (to ageing treatment) is concerned, Ti–29Nb–13Ta–4.6Zr is better than Ti–39Nb–13Ta–4.6Zr.

5. Conclusions

(1) Water quenching after solution treatment at 790°C for 1 h results in the formation of $\beta + \alpha''$ microstructure in Ti–29Nb–13Ta–4.6Zr but β phase in Ti–39Nb–13Ta–4.6Zr. Athermal ω phase particles could not be observed in both alloys, although the high Nb alloy shows stronger evidence of the displacive transformation that leads to ω_{ath} than the low Nb alloy.

(2) Both α and ω phase precipitate from the metastable β matrix in quenched Ti–29Nb–13Ta–4.6Zr alloy during isothermal ageing. Ageing between 600 and 350°C for 48 h results in α phase precipitation, and ageing between 400 and 300°C for 48 h results in the isothermal precipitation of ω phase.

(3) Ti–39Nb–13Ta–4.6Zr is more stable than Ti–29Nb–13Ta–4.6Zr with respect to diffusional reactions, and no definite evidence of α or ω phase was observed in the former alloy during short time isothermal ageing. The α phase particles that can be structurally identified were observed after longer time ageing (12 days) at both 500 and 400°C in Ti–39Nb–13Ta–4.6Zr.

(4) Ti–29Nb–13Ta–4.6Zr can be heat treated to obtain different microstructures and is better than Ti–39Nb–13Ta–4.6Zr as far as age hardenability is concerned.

Acknowledgements

The work has been supported by the NSFC (grant No. 59925103) and MoST of China (grant No. G2000067105). MN wishes to acknowledge the support of NEDO, JSPS, Ministry of Education, Science and Culture of Japan, Mitsubishi Foundation, Tokai Foundation, the Light Metal Education Foundation and the Iron and Steel Institute of Japan.

REFERENCES

- 1) K. Wang: *Mater. Sci. Eng. A* **213** (1996) 134–137.
- 2) R. Zwicker, K. Buehler, R. Mueller and L. J. Gustavson: in *Titanium '80, Science and Technology*, Proc. 4th Int. Conf. on Titanium, (Kyoto, May, 1980) pp. 505–514.
- 3) M. Semlitsch, F. Staub and H. Webber: *Biomed. Technik*. **30** (1985) 334–339.
- 4) P. Slanina, W. Frech, A. Bernhardson, A. Cedergren and P. Mattsson: *Acta Pharmacol. Toxicol.* **56** (1985) 331–336.
- 5) G. B. van der Voet, E. Marani, S. Tio and F. A. de Wolff: in *Aluminum Neurotoxicity: Histo and Cyto-Chemistry as a Tool in Environmental Toxicology*, eds. W. Graumann and J. Drukker (Fisher, Stuttgart, 1991) pp. 135–142.
- 6) Y. Song, D. S. Xu, R. Yang, D. Li, W. T. Wu and Z. X. Guo: *Mater. Sci. Eng. A* **260** (1999) 269–274.
- 7) Y. Song, R. Yang, Z. X. Guo and D. Li: in *Structural Biomaterials for the 21st Century*, eds. M. Niinomi, D. R. Lesuer, T. Okabe, H. E. Lippard and E. M. Taleff (TMS, Warrendale, PA, 2001) pp. 273–280.
- 8) M. Long and H. J. Rack: *Biomaterials* **19** (1998) 1621–1639.
- 9) M. Niinomi: *Mater. Sci. Eng. A* **243** (1998) 231–236.
- 10) K. Mishra, J. A. Davidson, R. A. Poggie, P. Kovacs and T. J. Fitzgerald: in *Medical Application of Titanium and Its Alloys: the Material and Biological Issues*, ed. J. E. Lemons, ASTM STP, Vol. 1272, (ASTM, West Conshohocken, PA, 1996) p. 96.
- 11) X. Tang, T. Ahmed and H. J. Rack: *J. Mater. Sci.* **35** (2000) 1805–1811.
- 12) H. Ledbetter and S. Datta: *Z. Metallkd.* **83** (1992) 195–198.
- 13) Z. Fan, P. Tsakiroopoulos and A. P. Miodownik: *Mater. Sci. Technol.* **9** (1993) 863–868.

- 14) Z. Fan, A. P. Miodownik and P. Tsakirooulos: *Mater. Sci. Technol.* **9** (1993) 1094–1100.
- 15) R. Boccaccini: *Z. Metallkd.* **88** (1997) 23–26.
- 16) E. W. Robare, C. M. Bugle, J. A. Davidson and K. P. Daigle: *Advances in the Science and Technology of Titanium Alloy Processing*, eds. L. Weiss, R. Srinivasan, P. J. Bania, D. Eylon and S. L. Semiatin (TMS, Warrendale, PA, 1997) pp. 283–291.
- 17) D. de Fontaine, N. E. Paton and J. G. Williams: *Acta Metall.* **19** (1971) 1153–1162.
- 18) D. de Fontaine: *Acta Metall.* **18** (1970) 275–279.
- 19) E. W. Collings: *Physical Metallurgy of Titanium Alloys*, (American Society for Metals, Metals Park, 1984).
- 20) D. L. Moffat and D. C. Larbalestier: *Metall. Trans. A* **19** (1988) 1677–1686.
- 21) J. M. Silcock, M. H. Davis and H. K. Hardy: *Mechanism of Phase Transformations in Metals, Institute of Metals Monograph No. 18*, (The Institute of Metals, London, 1956) pp. 93–104.
- 22) W. G. Burgers: *Physica* **1** (1934) 561–586.
- 23) L. Kaufman and H. Bernstein: *Computer Calculations of Phase Diagrams*, (Academic Press, New York, NY, 1970).
- 24) D. L. Moffat and D. C. Larbalestier: *Metall. Trans. A* **19** (1988) 1687–1694.
- 25) M. K. Koul and J. F. Breedis: *Acta Metall.* **18** (1970) 579–588.
- 26) G. H. Narayanan and T. F. Archbold: *Metall. Trans.* **1** (1970) 2281–2290.
- 27) Q. Y. Li: *Handbook of Non-ferrous Material Processing*, (Metallurgical Industry Press, Beijing, China, 1984) p. 48. (in Chinese).
- 28) Y. L. Hao, M. Niinomi, D. Kuroda, K. Fukunaga, Y. L. Zhou, R. Yang and A. Suzuki: Submitted to *Metall. Mater. Trans. A*.
- 29) Y. L. Hao, M. Niinomi, D. Kuroda, K. Fukunaga, Y. L. Zhou, R. Yang and A. Suzuki: *Metall. Mater. Trans. A* (in press).
- 30) Z. Fan: *Scripta Metall. Mater.* **29** (1993) 1427–1432.
- 31) K. Cho and J. Gurland: *Metall. Trans. A* **19** (1988) 2027–2040.